Understanding the Lévy ratchets in terms of Lévy jumps

J. Stat. Mech. (2013) P02007

(http://iopscience.iop.org/1742-5468/2013/02/P02007)

Journal of Statistical Mechanics: Theory and Experiment
An IOP and SISSA journal

Understanding the Lévy ratchets in terms of Lévy jumps

S A Ibáñez, S Risau-Gusman and S Bouzat

Consejo Nacional de Investigaciones Científicas y Técnicas, Centro Atómico Bariloche (CNEA), (8400) Bariloche, Río Negro, Argentina
E-mail: ibanezs@cab.cnea.gov.ar, srisau@cab.cnea.gov.ar and bouzat@cab.cnea.gov.ar

Received 10 September 2012
Accepted 7 December 2012
Published 1 February 2013

Online at stacks.iop.org/JSTAT/2013/P02007
doi:10.1088/1742-5468/2013/02/P02007

Abstract. We investigate the overdamped dynamics of a particle in a spatially periodic potential with broken reflection symmetry and subject to the action of a symmetric white Lévy noise. The system (referred to as the Lévy ratchet) has been previously studied using both Langevin and fractional Fokker–Planck formalisms, with the main find being the existence of a preferred direction of motion toward the steepest slope of the potential, producing a non-vanishing current. In this contribution we develop a semi-analytical study combining the Fokker–Planck and Langevin formalisms to explore the role of Lévy flights on the system dynamics. We analyze the departure positions of Lévy jumps that take the particle out of a potential well as well as the rates and lengths of such jumps, and we study the way in which long jumps determine the non-vanishing current. We also discuss the essential difference from the Gaussian-noise case (producing no current). Finally we study the current for different potential shapes as a function of the amplitude of the potential barrier. In particular, we show that standard Lévy ratchets produce a non-vanishing current in the infinite-barrier limit. This latter counterintuitive result can be easily understood in terms of the long Lévy jumps and analytically demonstrated.

Keywords: stochastic particle dynamics (theory), transport processes/heat transfer (theory), diffusion

1742-5468/13/P02007+18$33.00

Contents

1. Introduction

Directional transport in anisotropic spatially periodic systems captures the attention of many scientists due to its relevance for problems in physics [1, 2], biology [3], and technological applications [2]. The minimal models consider a particle in an external periodic potential with broken symmetry (the ratchet potential) and subject to the influence of a random or time-periodic signal generating the required nonequilibrium condition [2].

Recently, it has been shown [4, 5] that an additive symmetric Lévy noise [4]–[6] is enough to induce directional transport of particles in a static ratchet potential. Following that, several works have appeared providing further analysis of such a *Lévy ratchet* and studying different generalizations. Features such as inversions of current due to periodic modulation of the parameters [7], inertial effects [8], analysis of the weak-noise regime [9], analysis of the associated problem of the spatially tempered fractional Fokker–Planck equation [10], competition between Lévy forcing and a periodic a.c. driving [11], coexistence of Lévy flights and subdiffusion [12], and the effects of random flashing of the Lévy ratchet [13] have been addressed. The studies are motivated both by a pure theoretical interest on the Lévy systems and by the possible applications to plasma physics [5] and to the design of technological devices [2] as well. Lévy flights are relevant for many areas of science [5, 6] since they naturally emerge when modeling systems whose dynamics depend on the sum of independent random variables with long-tailed distributions. They appear in many different fields, ranging from physics and biology to social and economic sciences [5, 6].

The system studied in the pioneering papers [4, 5] obeys the following Langevin equation:

$$\frac{\mathrm{d}x}{\mathrm{d}t} = -V'(x) + \xi_{\alpha,\sigma}(t)\,. \tag{1}$$

J. Stat. Mech. (2013) P02007

Here, $-V'(x)$ is the force derived from the ratchet potential $V(x)$ and $\xi_{\alpha,\sigma}(t)$ is the white α-stable symmetric Lévy noise described below. The parameters α and σ satisfy $0 < \alpha \leq 2$ and $0 < \sigma$ and are called respectively the stability index and the scale factor of the Lévy noise [5, 6, 8]. In the limit $\alpha = 2$ the statistics of the noise becomes Gaussian and the equilibrium situation with vanishing current is recovered. In contrast, for $\alpha < 2$, the current is always non-vanishing and directed toward the steepest slope of the potential. Equation (1) can be numerically solved through the equivalent time discretized scheme [5, 8]

$$x(t_{i+1}) - x(t_i) = -V'(x(t_i))\,\mathrm{d}t + \sigma\,\mathrm{d}t^{1/\alpha} y(t_i), \tag{2}$$

with $i = 0, 1, 2, \ldots$ and $t_{i+1} - t_i = \mathrm{d}t$, while the $y(t_i)$ are independent random numbers distributed with the Lévy probability distribution $L_\alpha(y)$, defined through its Fourier transform as

$$L_\alpha(y) = \frac{1}{2\pi} \int_{-\infty}^{\infty} \mathrm{e}^{-\mathrm{i}ky} \exp\left[-|k|^\alpha\right] \mathrm{d}k. \tag{3}$$

For $\alpha < 2$ the Lévy noise is characterized by the existence of large fluctuations due to the fact that the distribution $L_\alpha(y)$ has long power-law tails decaying as $|y|^{1+\alpha}$ for $y \to \pm\infty$, so that the second moment diverges. This leads directly to a divergence of the mean square velocity for the ratchet system.

Using the Langevin approach, studies in [4] focus on the characterization of transport in situations for which not only the mean square velocity but even the mean velocity is divergent (as it occurs for $\alpha \leq 1$). New quantities characterizing directionality and spreading of particles are introduced and studied as functions of the system parameters. The work in [5] provides both Langevin and Fokker–Planck results focusing on the region $\alpha > 1$ where the current is well defined. Meanwhile, in [9], the authors study the system in the weak-noise limit ($\sigma \to 0$) and provide analytical results for the current and the splitting probabilities in such a limit, among other quantities of interest. The analysis is performed using the method of decomposition developed in [14, 15], which considers the white Lévy noise as composed by a Gaussian-like noise (i.e. with finite variance) plus a Poisson process describing the large impulses. The authors show that, for $\sigma \to 0$, the current is produced by long Lévy jumps departing form the minimum of the potential and taking the particle out of the potential well.

In this contribution we develop a semi-analytical study combining the Fokker–Planck and Langevin formalisms to explore the role of Lévy flights on the dynamics of the Lévy ratchet for arbitrary values of σ considering $1 < \alpha \leq 2$. We study the rates and departure positions of Lévy jumps that take the particle out of a potential well for different values of α and σ. We provide generalizations for finite σ of some of the results given in [9], including probabilities for long jumps between distant potential wells, and we analyze the way in which long jumps determine the non-vanishing current. Finally, in the last part of the paper we study the current for different potential shapes as a function of the amplitude of the potential barrier. In particular, we show that standard Lévy ratchets produce non-vanishing currents in the infinite-barrier limit. This latter rather counterintuitive result can be easily understood in terms of the long Lévy jumps.

The paper is organized as follows. In section 2 we give an overview of the previous developed Fokker–Planck formalism. Section 3 contains the main analysis of the nature and role of Lévy flights in ratchets and the way in which they produce the non-vanishing

J. Stat. Mech. (2013) P02007

current. In section 4 we study the dependence of the current on the amplitude of the potential barrier as well as the infinite-barrier limit. Section 5 is devoted to discussion and conclusions.

2. The Fokker–Planck (FP) formalism

Throughout the paper, we will use results for the current and the stationary distribution of the Lévy ratchet calculated using a Fokker–Planck formalism previously developed for studying the more general problem of a Lévy ratchet with flashing potential [13]. Here we present an overview of the formalism indicating the way in which the mentioned quantities are calculated.

We consider the Langevin equation (1) with a periodic potential $V(x)$ with period L. The corresponding Fokker–Planck equation (FPE) can be written as [5, 13]:

$$\partial_t P(x,t) = \partial_x (P(x,t)\partial_x V(x)) + \sigma^\alpha \partial_x^\alpha P(x,t). \tag{4}$$

Here, $\partial_x^\alpha \equiv \partial^\alpha/\partial|x|^\alpha$ stands for the Riesz–Feller fractional derivative of order α [16].

We focus on the stationary problem in which $\partial_t P(x,t) = 0$, and we look for a periodic stationary solution $P_{\rm s}(x)$ normalized in one period of the potential. We use the Fourier method developed in [13] for the more general system of a Lévy ratchet with random flashing. Considering the discrete Fourier transform $f(x) = \sum_j \tilde{f}_j \exp(\mathrm{i}q_j x)$, with $q_j \equiv 2\pi j/L$, integer j and $\tilde{f}_j = \int_0^L (\mathrm{d}x/L)\, f(x) \exp(-\mathrm{i}q_j x)$, we get the following equations for the Fourier amplitudes $\tilde{P}_{{\rm s},k}$ of $P_{\rm s}(x)$:

$$-q_k \sum_{j\neq k} q_j \tilde{V}_j \tilde{P}_{{\rm s},k-j} - \sigma^\alpha |q_k|^\alpha \tilde{P}_{{\rm s},k} = q_k^2 \tilde{V}_k \qquad (k \neq 0). \tag{5}$$

The linear system (5) is then solved by considering a large number of modes (typically 500–5000) and checking convergence. Note that the normalization condition implies $\tilde{P}_{{\rm s},0} = 1$. Finally the stationary current is computed as [13]:

$$J \equiv J_0 = -i \sum_j q_j \tilde{V}_j \tilde{P}_{{\rm s},-j}. \tag{6}$$

3. Lévy jumps in the Lévy ratchet

Here we investigate the characteristics of the Lévy jumps in the stationary regime of the ratchet system described by equations (1) and (4) in order to analyze their role in determining the current. We consider the standard ratchet potential

$$V(x) = \frac{V_0}{2\pi}\left[\sin\left(2\pi\frac{x+x_0}{L}\right) + \frac{1}{4}\sin\left(4\pi\frac{x+x_0}{L}\right)\right] \tag{7}$$

with period $L = 1$, shown in figure 1. Here, V_0 controls the amplitude of the potential while the parameter $x_0 = \cos^{-1}[(1+3^{1/2})^{1/2}/2]/\pi \simeq 0.19$ is included to shift the maxima to the integer positions. Each of the regions between two maxima of the potential (i.e. $k < x < k+1$, with integer k) will be referred to as a *potential well*. The minima of the potential are located at $x_{\rm min} = 1 - 2x_0 + k \simeq 0.62 + k$ with integer k.

J. Stat. Mech. (2013) P02007

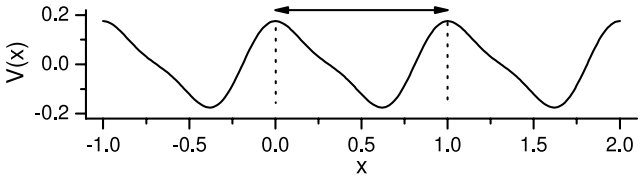

Figure 1. Ratchet potential $V(x)$ of equation (7) for $V_0 = 1$. The double arrow and the vertical segments indicate the potential well $0 < x < 1$ usually considered as reference.

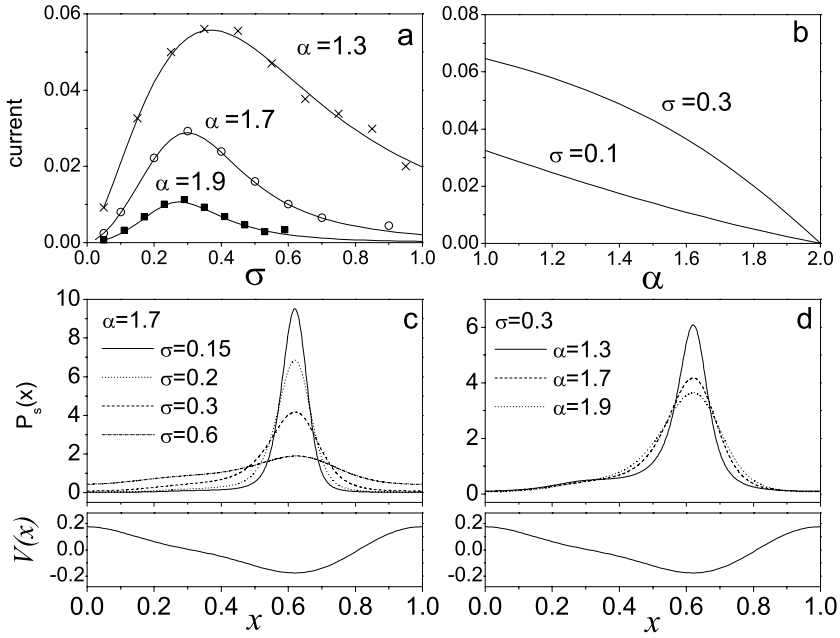

Figure 2. (a) Fokker–Planck solution (solid lines) and Langevin results (symbols) for the current J as a function of σ for different values of α. (b) Fokker–Planck solution for J as function of α. (c) and (d) show Fokker–Planck results for the stationary distributions $P_{\rm s}(x)$. The potential profile of $V(x)$ is shown below panels (c) and (d) for the sake of guidance. All calculations are for $V_0 = 1$.

As a starting point, in figures 2(a) and (b) we show the Fokker–Planck and Langevin results for the current J as function of σ and α, which are known from previous works [4, 5], while figures 2(c) and (d) show the distribution $P_{\rm s}(x)$ for different values of α and σ, together with the potential $V(x)$. Importantly, in figure 2(a) we see that, at fixed α, there exists an optimal value of σ maximizing the current. This is related to a common effect in most systems producing noise induced transport. Namely, small levels of noise produce low transport because the transitions between different potential wells are unlikely. Meanwhile, high levels of noise 'rub out' the potential and lead also to very small currents. Hence, the larger transport effects occur at intermediate levels of noise. Figure 2(b) shows that the current decreases monotonically with α at constant σ, as found in previous works [4, 5]. To complete this overview of the dependence of J on the Lévy noise parameters, it is worth mentioning that when computing J as a function of α at a constant value of the

J. Stat. Mech. (2013) P02007

noise intensity $\chi = \sigma^\alpha$ (instead of constant σ), an optimum value of $\alpha > 1$ is observed for small enough values of χ [5].

To investigate Lévy jumps, we now focus on the discretized Langevin scheme of equation (2). We consider a particle located in the well $0 < x < 1$. For simplicity we note $x_i = x(t_i)$ and $y_i = y(t_i)$. At time t_i, the particle performs a jump of length $\Delta x_i = x_{i+1} - x_i$ determined by equation (2). The distribution of jump lengths $P_{\rm jump}(x_i, \Delta x)$ can be calculated from equation (2) taking into account the distribution for y_i and the relation $P_{\rm jump}(x_i, \Delta x)\,{\rm d}(\Delta x) = L_\alpha(y_i)\,{\rm d}y_i$. We get

$$P_{\rm jump}(x_i, \Delta x) = \frac{1}{\sigma\,{\rm d}t^{1/\alpha}} L_\alpha\left(\frac{\Delta x + V'(x_i)\,{\rm d}t}{\sigma\,{\rm d}t^{1/\alpha}}\right). \tag{8}$$

3.1. Departing positions and rates for escapes from a potential well

The current on the Lévy ratchet is expected to be due to asymmetries in the probabilities for right and left jumps between different potential wells. In order to understand the details of the transport mechanism we thus analyze the statistical properties of such jumps. In what follows, a Lévy jump taking the particle out of a potential well (in a single time step) will be referred to as *an escape*. We will speak of right or left escapes, according to the corresponding value of Δx being positive or negative, respectively. Let us first study the rates and departing positions for right and left escapes.

For a particle located at x_i at time t_i in the well $0 < x_i < 1$, the probability of jumping to a position $x_{i+1} > 1$ (i.e. to any of the potential wells located at the right of the original one) is simply computed by integrating $P_{\rm jump}(x_i, \Delta x)$ on Δx between $1 - x_i$ and ∞. This gives $1 - F_\alpha((1 - x_i + V'(x_i)\,{\rm d}t)/(\sigma\,{\rm d}t^{1/\alpha}))$, where $F_\alpha(u) = \int_{-\infty}^{u} L_\alpha(y)\,{\rm d}y$. Equivalently, the probability of jumping to a position $x_{i+1} < 0$ (i.e. to any of the wells on the left) is computed by integrating $P_{\rm jump}(x_i, \Delta x)$ on Δx between $-\infty$ and $-x_i$. This gives $F_\alpha((-x_i + V'(x_i)\,{\rm d}t)/(\sigma\,{\rm d}t^{1/\alpha}))$.

Now, dividing by ${\rm d}t$ the previous expressions for escape probabilities and considering that in the stationary regime the position of the particle is distributed according to the stationary distribution $P_{\rm s}(x)$, we can compute the rates for right and left escapes departing from position x, referred to as $R_+(x)$ and $R_-(x)$, respectively. We get:

$$\begin{aligned} R_+(x) &= \frac{1}{{\rm d}t} P_{\rm s}(x)\left(1 - F_\alpha\left(\frac{1 - x + V'(x)\,{\rm d}t}{\sigma\,{\rm d}t^{1/\alpha}}\right)\right) \\ R_-(x) &= \frac{1}{{\rm d}t} P_{\rm s}(x)\left(F_\alpha\left(\frac{-x + V'(x)\,{\rm d}t}{\sigma\,{\rm d}t^{1/\alpha}}\right)\right). \end{aligned} \tag{9}$$

In figure 3 we analyze the functions $R_+(x)$ and $R_-(x)$ for fixed values of α and σ. We focus on the behavior of $R_\pm(x)$ at small but non-vanishing ${\rm d}t$, which characterizes the jumps in actual numerical simulations and we also study their ${\rm d}t \to 0$ limits and their symmetry properties.

Figure 3(a) shows results for $R_+(x)$ considering the value ${\rm d}t = 0.001$ typically used in Langevin simulations [4, 5, 8]. We see that $R_+(x)$ attains nonnegligible values mainly in two well-defined zones of the domain $0 < x < 1$. One located around the minimum of the potential ($x_{\rm min} \simeq 0.62$), and the other at $x \lesssim 1$, close to the maximum of the potential. This means that right escapes from the well $0 < x < 1$ to a position $x > 1$ depart mainly from two such zones. The peak at $x = 1$ is simply due to the fact that, for $x \lesssim 1$, although

J. Stat. Mech. (2013) P02007

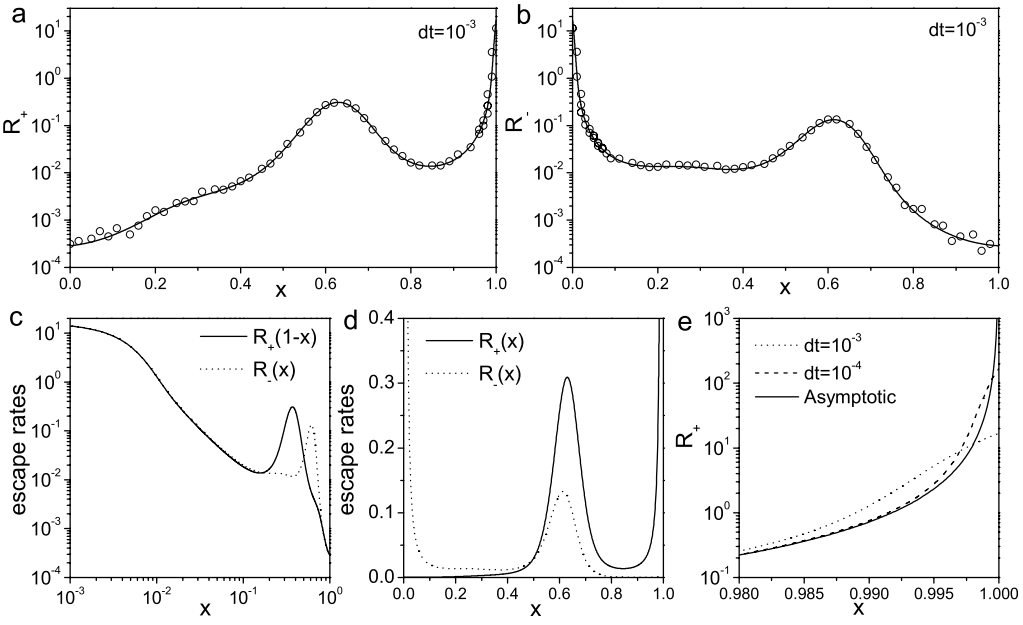

Figure 3. Escape rates for $\alpha = 1.7$ and $\sigma = 0.2$. (a) Rate for right escapes ($R_+(x)$) for $\mathrm{d}t = 10^{-3}$. The solid line shows results from equation (9) while symbols comes from Langevin simulations. (b) Ibid panel (a) for $R_-(x)$. (c) Behavior of $R_+(1-x)$ and $R_-(x)$ for $\mathrm{d}t = 10^{-3}$ showing the coincidence of both rates in the region close to the maximum of the potential. (d) Results for $R_+(x)$ and $R_-(x)$ in linear scale for $\mathrm{d}t = 10^{-3}$. (e) Escapes rate $R_+(x)$ for different values of $\mathrm{d}t$ and for the asymptotic ($\mathrm{d}t \to 0$) limit.

the probability of finding the particle is low, very small Lévy impulses (i.e. highly likely impulses) are enough to take the particle to the right of the well. Conversely, the maximum of $R_+(x)$ at the potential minimum is due to the fact that, although large (relatively unlikely) impulses are needed, the probability of finding the particle in such a region is high. Analogously, $R_-(x)$ has only relevant contributions at $x \sim x_{\min}$ and $x \gtrsim 0$ (see figure 3(b)). Thus, left escapes depart mainly from the neighborhoods of two such points.

Interestingly, the peak of $R_+(x)$ at $x = 1$ and that of $R_-(x)$ at $x = 0$ are symmetric to each other, as is better shown in figure 3(c), where we plot $R_+(1-x)$ together with $R_-(x)$ as function of x. This symmetry indicates that the small right escapes (departing from $x \lesssim 1$) are statistically canceled with small left escapes departing from $x \gtrsim 0$. Thus, the positive current has to be sustained by large escapes departing from zones not too close to the maxima of the potential, where $R_+(x)$ and $R_-(x)$ differ each other. The main asymmetry occurs in the region between $x \sim 0.4$ and $x \sim 0.8$, as it is better appreciated in figure 3(d), where we show $R_+(x)$ and $R_-(x)$ in linear scales. The dominance of right escapes is apparent. Note that the asymmetry of the position of the minimum of the potential $x_{\min}$ with respect to the right ($x = 1$) and left ($x = 0$) maxima appears as the main origin of the dominance of $R_+(x)$, since it implies that shorter (i.e. more likely) jumps are needed for escaping to the right than for escaping to the left from the zone where $P_{\mathrm{s}}(x)$ is maximal. However, as we later show, such asymmetry in the position of $x_{\min}$ is not strictly necessary to obtain a non-vanishing current.

doi:10.1088/1742-5468/2013/02/P02007

J. Stat. Mech. (2013) P02007

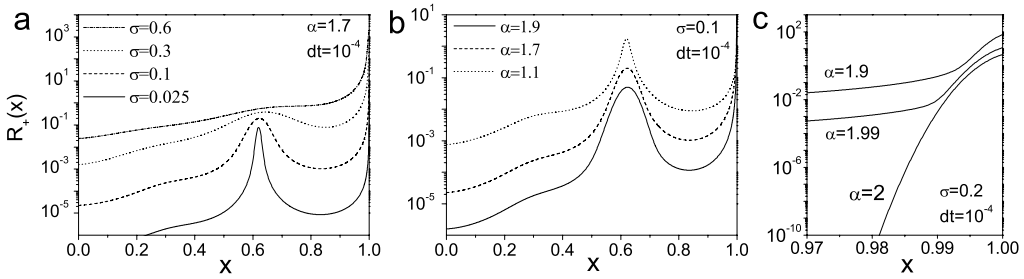

Figure 4. Dependence of the right escape rate $R_+(x)$ on the parameters of the Lévy noise. (a) Results for different values of σ at fixed α and dt. (b) Results for different values of α at fixed σ and dt. (c) Behavior for $x \lesssim 1$ when approaching to the Gaussian-noise limit.

The limits for d$t \to 0$ of $R_\pm(x)$ can be calculated using the asymptotic formula $F_\alpha(x) \simeq 1 - k_\alpha x^{-\alpha}$ valid for large x, with $k_\alpha = \Gamma(\alpha)\sin(\pi\alpha/2)/\pi$. We get $R_+(x) \to P_\mathrm{s}(x)(\sigma^\alpha k_\alpha/(1-x)^\alpha)$ and $R_-(x) \to P_\mathrm{s}(x)(\sigma^\alpha k_\alpha/x^\alpha)$ for d$t \to 0$. Thus, in the asymptotic limit, the functions $R_+(x)$ and $R_-(x)$ diverge at $x = 1$ and $x = 0$, respectively. Nevertheless, the symmetry between right and left jumps departing from zones close to the maximum of the potential keeps valid. The divergences can be understood as follows. Consider for instance a particle situated in a small neighborhood of $x = 1$. Clearly, for arbitrary small values of dt, the position of the particle would fluctuate arbitrarily fast between $x < 1$ and $x > 1$ driven by small instances of the noise, until a large enough Lévy impulse takes it away from the neighborhood of the maximum. Hence, an arbitrarily high rate of escapes would be observed. Nevertheless, clearly such escapes do not contribute to the current.

The convergence of $R_\pm(x)$ in the d$t \to 0$ limit is relatively fast, except for the region close to the divergences. This can be seen in figure 3(e), where we show $R_+(x)$ for different values of dt together with the asymptotic results in the zone close to $x = 1$. It is worth mentioning that in the scales of the figures 3(a)–(c), the d$t = 10^{-3}$ and d$t \to 0$ escape rates are indistinguishable. We should also mention that, in order to evaluate the distributions $R_\pm(x)$ from equation (9) at finite dt, we used the FP solution for $P_\mathrm{s}(x)$. This is actually an approximation, since we should have considered finite dt stationary distributions. However, we find that the Langevin results for $P_\mathrm{s}(x)$ converge very rapidly to the FP distribution and the approximation is practically exact for d$t \lesssim 10^{-3}$. Moreover, the goodness of the approximation is also evident from the matching between Langevin and FP results for $R_\pm$ in figure 3.

Let us now analyze the dependence of the escape rates on the Lévy noise parameters σ and α. For simplicity, we focus on the behavior of $R_+(x)$ since the results for $R_-(x)$ are analogous. Figure 4(a) shows results for $R_+(x)$ at different values of σ. We see that, as σ is decreased, the peak of $R_+(x)$ at x_min gets narrower due to the behavior of $P_\mathrm{s}(x)$. Thus, for $\sigma \to 0$, we expect a delta-like profile. This is in agreement with what is discussed in [9]. Concerning the behavior of $R_+(x)$ at large σ, we see that the peak at x_min becomes flat and eventually disappears. This is just because the stationary distribution $P_\mathrm{s}(x)$ gets flat (see figure 2(c)).

Figure 4(b) shows results for $R_+(x)$ for different values of α at fixed dt. We see that $R_+(x)$ decreases in all the spatial domain with increasing α. This is to be expected since the probability of large jumps decreases with α. Figure 4(c) shows a detail of the

J. Stat. Mech. (2013) P02007

behavior of $R_+(x)$ close to $x = 1$ as α approaches the Gaussian-noise case. The abrupt change between the results for $\alpha = 1.99$ and those for $\alpha = 2$ is remarkable. It can be seen that only the peak at $x = 1$ survives in the Gaussian limit. This can be demonstrated analytically since, interestingly, for $\alpha = 2$ the function F_α is analytical. In fact, we have $F_2(u) = (1 + \mathrm{Erf}(u/2))/2$, and we are able to demonstrate the following properties for $R_+(x)$: (i) $\lim_{\mathrm{d}t\to 0} R_+(x) = 0$ for $0 \leq x < 1$, (ii) $\lim_{\mathrm{d}t\to 0} R_+(1) = \infty$. Thus, $R_+(x)$ behaves as the left branch of a delta function at $x = 1$. This simply means that, for $\alpha = 2$, in the limit $\mathrm{d}t \to 0$, any particle going from a $x < 1$ to $x > 1$ has to pass by the point $x = 1$, in contrast to what happens for $\alpha < 2$. The properties of $R_-(x)$ for $\alpha = 2$ are completely analogous to those of $R_+(x)$. This means, $R_-(x)$ vanishes for $x > 0$ and has a delta-like behavior at $x = 0$. Moreover, the symmetry between the peaks of R_+ at $x \lesssim 1$ and that of R_- at $x \gtrsim 0$ found for $\alpha < 2$ is still valid for $\alpha = 2$. This leads directly to the vanishing of the current for $\alpha = 2$, since no large escapes are present, while right and left small escapes cancel each other.

3.2. Jumps between distant wells, asymmetries and splitting probabilities

We have just analyzed the departing positions and rates for right and left escapes from a potential well with no consideration of the well at which the particle arrives. Here we analyze this latter point and show that usually the main left–right asymmetries appear in the jumps of one potential period length.

For a particle in the stationary regime, let us consider the probability P_k of jumping in a single time step to a position located k wells to the right of the original well. Analogously, for the left escapes we consider negative values of k. The probabilities P_k can be computed by integrating $P_{\mathrm{jump}}(x, \Delta x)$ on the appropriate intervals of Δx and weighting all the possible departure positions. We get

$$P_k = \int_0^1 \mathrm{d}x\, P_{\mathrm{s}}(x) \int_{k-x}^{k+1-x} P_{\mathrm{jump}}(x, \Delta x)\, \mathrm{d}(\Delta x) \tag{10}$$

for integer $k \neq 0$. This can be written in terms of the Lévy function F_α as

$$P_k = \int_0^1 \mathrm{d}x\, P_{\mathrm{s}}(x) \left(F_\alpha \left(\frac{k + 1 - x + V'(x)\,\mathrm{d}t}{\sigma\, \mathrm{d}t^{1/\alpha}} \right) - F_\alpha \left(\frac{k - x + V'(x)\,\mathrm{d}t}{\sigma\, \mathrm{d}t^{1/\alpha}} \right) \right). \tag{11}$$

For $k \neq \pm 1$, the rates $P_k/\mathrm{d}t$ are independent of $\mathrm{d}t$ for small enough $\mathrm{d}t$ as a consequence of the self-similarity of the Lévy functions, as happens with the rates $R_\pm(x)$. Importantly, this does not occur for $k = \pm 1$ since, with the definitions in equation (10), $P_{\pm 1}$ diverge for $\mathrm{d}t \to 0$ due to the same effect explained for the divergence of $R_\pm(x)$ at the maxima of the potential, related with the existence of very small left and right escapes which do not contribute to the current. We can overcome this problem by introducing a minimal cut-off δ for the lengths of the jumps, and considering only jumps with $|\Delta x| > \delta$, with $1 \gg \delta > 0$. We stress that this is only necessary for $k = \pm 1$. We get

$$\begin{aligned} P_1 &= \int_0^1 \mathrm{d}x\, P_{\mathrm{s}}(x) \left(F_\alpha \left(\frac{2 - x + V'(x)\,\mathrm{d}t}{\sigma\, \mathrm{d}t^{1/\alpha}} \right) - F_\alpha \left(\frac{\mathrm{Max}(\delta, 1 - x) + V'(x)\,\mathrm{d}t}{\sigma\, \mathrm{d}t^{1/\alpha}} \right) \right) \\ P_{-1} &= \int_0^1 \mathrm{d}x\, P_{\mathrm{s}}(x) \left(F_\alpha \left(\frac{\mathrm{Min}(-\delta, -x) + V'(x)\,\mathrm{d}t}{\sigma\, \mathrm{d}t^{1/\alpha}} \right) - F_\alpha \left(\frac{-1 - x + V'(x)\,\mathrm{d}t}{\sigma\, \mathrm{d}t^{1/\alpha}} \right) \right). \end{aligned} \tag{12}$$

J. Stat. Mech. (2013) P02007

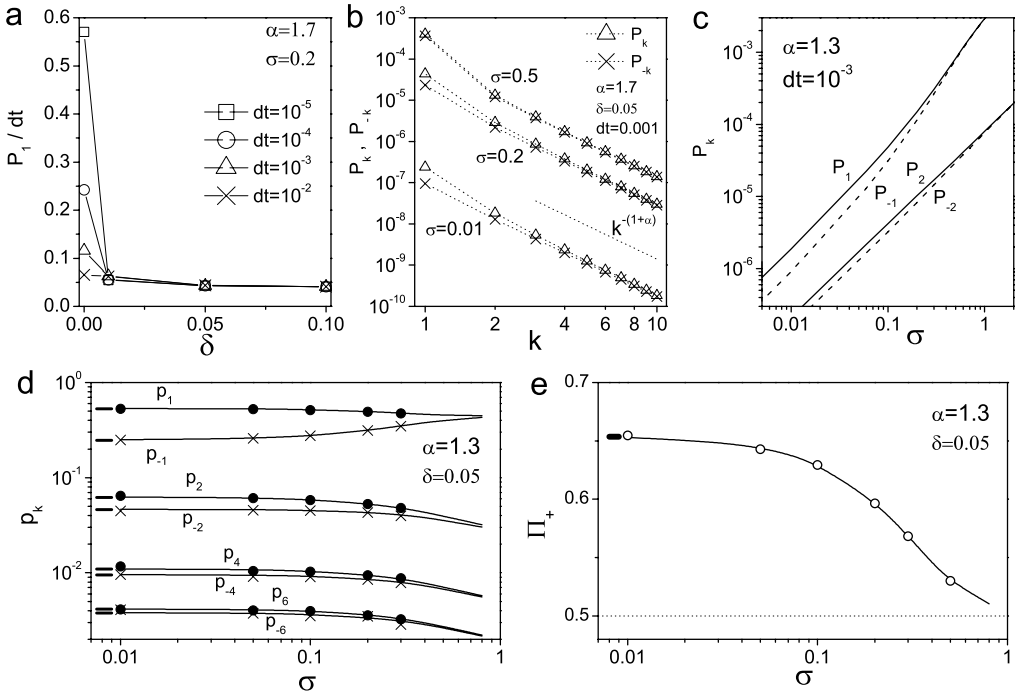

Figure 5. Probabilities for jumps between distant wells. (a) Rate for right one-well escapes as function of δ for different values of dt. (b) P_k and P_{-k} versus k for different values of σ. (c) P_1, P_{-1}, P_2 and P_{-2} as a function of σ. (d) Conditional probabilities p_k as a function of σ. The symbols represent Langevin results while solid lines correspond to the semi-analytical theory. The short black segments on the left indicate the $\sigma \to 0$ limit calculated with the analytical formula given in [9]. (e) Right splitting probability Π_+ as a function of σ. The symbols represent Langevin results while solid lines correspond to the semi-analytical theory. The short segments on the left are the analytical $\sigma \to 0$ result from [9]. All the results in panels (a)–(c) come from the semi-analytical theory.

Although these definitions are somehow arbitrary due to the existence of the cut-off, they are useful to understand the way in which escapes of different lengths contribute to the current, as we later show. For practical purposes, the value of δ can be chosen in the region where we have $R_+(1-\delta) \simeq R_-(\delta)$, so that we only discard short-length escapes which are compensated by other short-length escapes in the opposite direction. For instance, for the system studied in figure 3 (see figure 3(c)), any value $\delta \lesssim 5 \times 10^{-2}$ would work well. This is shown in figure 5(a), where we plot $P_1/\mathrm{d}t$ as a function of δ for different values of dt. We see that we can find a relatively wide region of δ for which P_1 depends very smoothly on δ. Moreover, $P_1/\mathrm{d}t$ is independent of dt.

In figure 5(b) we show P_k as a function of k for different values of σ. As expected, we see that P_k grows with σ (for fixed k) and decays as $k^{-(1+\alpha)}$ for large k (following the decay law of L_α). Figure 5(c) shows P_k as a function of σ for $k = \pm 1$ and ± 2. We can see that the strongest asymmetry occurs for the case $k = 1$. Therefore, we expect that the main contribution to the current will come from one-well length escapes. This will be confirmed in section 3.3, where we study different approximations to the current.

J. Stat. Mech. (2013) P02007

The probabilities P_k can be normalized to get conditional probabilities p_k of jumping k wells to the right in a single step given that the particle escapes from the original well in such a time step. We get

$$p_k = \frac{P_k}{Z_\Pi} \tag{13}$$

for $k \neq 0$, with $Z_\Pi = \sum_{k\neq 0} P_k$. These conditional probabilities result as natural extensions for finite σ of the conditional probabilities defined for $\sigma \to 0$ in [9] of jumping k wells given the occurrence of a *spike* (i.e. a Lévy impulse surpassing a certain threshold [9]). In figure 5(d) we show p_k as function of σ for several values of k. We see that, for small enough σ, the numerical values found for p_k match the analytical results found in [9].It is also interesting to see that p_{-1} grows with σ while every other p_k decreases. Thus, as σ increases, the probability of escaping one well to the left grows at the expense of the probabilities of escaping to any other well, and mainly due to the decreasing of p_1. This is the origin of the decrease of the current at large σ and is due to the broadening of $P_s(x)$, also observable in the broadening of $R_\pm(x)$ (see figures 2(c) and 4(a)).

Finally, by summing up the conditional probabilities p_k we can generalize the *splitting probabilities* $\Pi_+ = \sum_{k=1}^{\infty} p_k$ and $\Pi_- = 1 - \Pi_+$ defined in [9] for $\sigma \to 0$, now considering arbitrary values of σ. In figure 5(e) we show Π_+, which in the $\sigma \to 0$ coincide with the analytical value provided in [9].

3.3. Recovering the current from the jumps between wells

Here we show how the current can be recalculated by considering the jumps between distant wells through the probabilities P_k defined in section 3.2.

Assuming that the relaxation processes within a given potential well are rapid compared with the occurrence of jumps between wells, we can consider that a jump of k potential wells to the right produces a contribution to the current equal to $kL/\mathrm{d}t$ (with $L = 1$ the period of the potential) in the corresponding time step. Here, we have replaced the actual length of the jump Δx, which for a right k-wells jump satisfies $(k-1)L < \Delta x < (k+1)L$, by the effective or average contribution kL found after the relaxation process. The same can be done for left k-well jumps considering negative values of k.

With these assumptions, the current can be approximated as:

$$J_\mathrm{A} = \frac{L}{\mathrm{d}t} \sum_{k=1}^{\infty} k(P_k - P_{-k}). \tag{14}$$

In order to analyze the contributions to the current of the escapes of different lengths we can consider only jumps with $|k| \leq M$ and compute the restricted sum

$$J_\mathrm{A}^M = \frac{L}{\mathrm{d}t} \sum_{k=1}^{M} k(P_k - P_{-k}). \tag{15}$$

In figure 6 we show J_A^M for different values of M together with the exact FP solution for J as function of σ for $\alpha = 1.3$ and 1.7. We see that J_A^M provide good approximations for the current. Even the case $M = 1$ represents a reasonably good approximation for low and intermediate values of σ, almost up to the region where J is maximized. This means

J. Stat. Mech. (2013) P02007

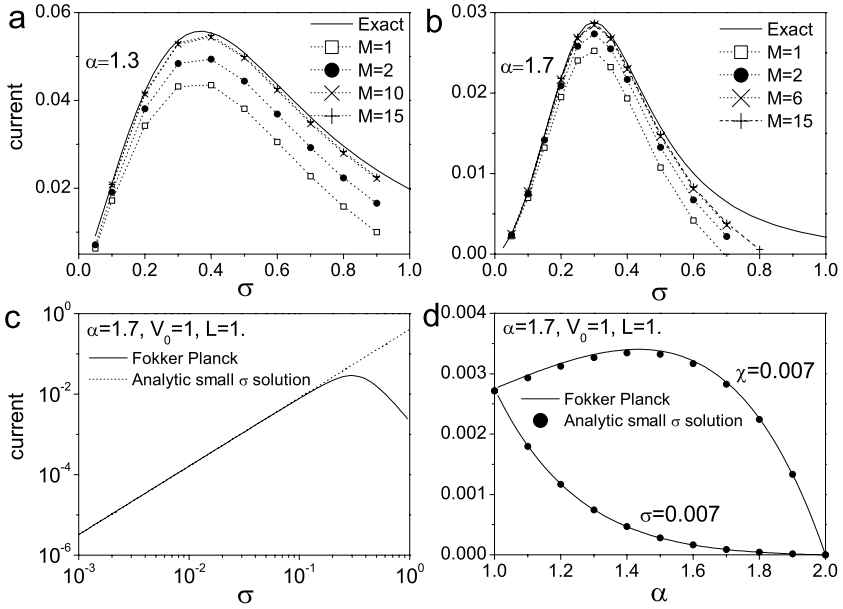

Figure 6. Approximations to the current. (a) Exact FP solution for the current (solid line) and approximation J_{A}^{M} for different values of M (dotted and lines with symbols) as functions of σ for $\alpha = 1.3$. (b) Ibid panel (a) for $\alpha = 1.7$. (c) Analytic $\sigma \to 0$ approximation together with FP results for J as a function of σ. (d) Analytic $\sigma \to 0$ approximation together with FP results for J as a function of α at constant $\sigma = 0.007$ and at constant $\chi = \sigma^{\alpha} = 0.007$.

that in such a region of parameters the dynamics is dominated by one-well jumps, as suggested in section 3.2. For increasing σ or decreasing α, due to the existence of larger jumps, an increasing number of terms is needed in J_{A}^{M} to get a good approximation for J. Nevertheless, it can be seen that J_{A}^{M} does not converge to the actual current for $M \to \infty$ for large enough σ. For instance, in the case $\alpha = 1.7$, we see that the results for $M = 6$ and 15 are indistinguishable and still different from the Fokker–Planck current. The origin of such difference has to be ascribed to the assumption of integer values for the jumps considered in the definition of J_{A}. In fact, it is to be expected that such an assumption does not hold for large values of σ or small values α since these conditions favor large jumps, and thus the relaxation processes may not result as being so rapid in comparison with the occurrence of jumps between wells. Note that the consideration of a finite dt for computing J_{A}^{M} is not a reason for the difference between J_{A}^{M} and J, since Langevin simulations with the same dt match the FP solution.

The results in figure 6 help us to get a deeper insight on the existence of an optimal σ maximizing J at fixed α. Clearly, this effect is well described by the approximation J_{A}^{1}, so it can be analyzed in terms of one-well escapes. We focus on the case $\alpha = 1.3$ shown in figure 6(a). Note that J_{A}^{1} is proportional to the difference between the curves for P_1 and P_{-1} depicted in figure 5(c). In view of this, it is easy to understand that the increasing of J with σ at small σ is due to the fact that P_1 and P_{-1} grow with approximately the same power law of σ. This clearly implies that $P_1 - P_{-1}$ increases with σ. Meanwhile, the decreasing of the current at large σ is due to, in such a region, P_{-1} growing faster than

J. Stat. Mech. (2013) P02007

P_1 so that $P_1 - P_{-1}$ decreases. The decreasing of the current at large σ is also related to the decreasing of Π_+ shown in figure 5(c).

For small σ, where the approximation J_A works well, we can go further in our analysis and connect with the results in [9]. Note that for $\sigma \to 0$ the approximation J_A is expected to become exact since, in such a limit, the probability distribution $P_s(x)$ approaches a Dirac delta centered at x_{min} and, thus, the contributions to the current of the jumps between wells become exact integer multiples of L/dt. Let us now investigate the approximation J_A in such a regime of small σ assuming that $P_s(x)$ is well approximated by $\delta(x - x_{min})$. With this assumption, we can easily perform the integration in equation (11) to get

$$P_k = F_\alpha\left(\frac{k+1-x_{min}+V'(x_{min})\,dt}{\sigma\,dt^{1/\alpha}}\right) - F_\alpha\left(\frac{k-x_{min}+V'(x_{min})\,dt}{\sigma\,dt^{1/\alpha}}\right). \tag{16}$$

Replacing this in equation (14), we can compute the $dt \to 0$ limit of J_A by using the asymptotic formulas for F_α given in section 3.1, and considering $F(y) = 1 - F(-y)$ for $y \to -\infty$. We get

$$\begin{aligned} J &= \sigma^\alpha k_\alpha \sum_{n=1}^{\infty} n\left[(n-x_{min})^{-\alpha} - (1+n-x_{min})^{-\alpha} - (n-1+x_{min})^{-\alpha} + (n+x_{min})^{-\alpha}\right] \\ &= \sigma^\alpha k_\alpha \sum_{n=0}^{\infty} (n-x_{min}+1)^{-\alpha} - (n+x_{min})^{-\alpha} \\ &= \sigma^\alpha k_\alpha \left[\zeta(\alpha, 1-x_{min}) - \zeta(\alpha, x_{min})\right]. \end{aligned} \tag{17}$$

Here, $\zeta(\alpha, x)$ is the Hurwitz zeta function (a generalization of the Riemann's zeta function), while $k_\alpha = \Gamma(\alpha)\sin(\pi\alpha/2)/\pi$ as defined in section 3.1. In order to analyze the dependence of this solution on all the system parameters it is worth considering the more general situation of an arbitrary period L for the ratchet potential in equation (7). Then, defining the asymmetry parameter $q = x_{min}/L$ (where now $0 < x_{min} < L$ is the position of the minimum), it is straightforward to show that the result in equation (17) becomes

$$J = \sigma^\alpha k_\alpha \left[\zeta(\alpha, 1-q) - \zeta(\alpha, q)\right] L^{1-\alpha}. \tag{18}$$

This analytical result for the current is the same as that found in [9], where the authors studied the $\sigma \to 0$ limit by a different procedure[1]. Note, however, that here we have particularized for the case of zero chirality of the Lévy noise ($\beta = 0$). In order to understand the agreement between our result and that in [9], a very important point has to be remarked. Namely, the result in equation (18) depends neither on the potential amplitude V_0 nor on the detailed shape of the potential. The only relevant parameters concerning the potential are the period L and the asymmetry parameter q. This is the reason why we have found the same result as in [9] in spite of having considered a different functional form for the potential. Note that, once we have set $P_s(x) = \delta(x - x_{min})$, only the distances L and x_{min} matter, but not the values of the potential. This is so because, according to equation (8), the lengths of the Lévy jumps depend only on the derivative of the potential at the departing position, but not on the values of the potential between the departing position and the arriving position. Thus, when $P_s(x)$ is delta shaped, as all

[1] To see the agreement between our formula (18) and that given in [9] it is important to note that the constant k_α can also be written as $k_\alpha = (2\alpha|\cos(\pi\alpha/2)\Gamma(-\alpha)|)^{-1}$. Moreover, note that there are some typos in equation (12) of [9] that affect the calculation of the current.

J. Stat. Mech. (2013) P02007

the escapes depart from $x_{\min}$, the escape probabilities are not conditioned by the details of the potential. In contrast, for larger values of σ, the current does depend on V_0 since the escapes can depart from any position with different probabilities which depend on the details of $V(x)$. The independence of J on V_0 at small σ will be further analyzed in section 4 from another point of view.

As expected, the agreement between the result in equation (18) and the Fokker–Planck solution for the current is complete at small enough σ. This can be seen in figure 6(c), where we show both results plotted versus σ at fixed $\alpha = 1.7$. Meanwhile, figure 6(d) shows that the equation (18) correctly describes the decreasing of J with α at constant (small) σ, as well as the nonmonotonic behavior found at constant (small) noise intensity $\chi = \sigma^{\alpha}$, mentioned at the beginning of section 3 [5].

4. The infinite-barrier limit

As we indicated in section 3, according to equation (8), the lengths of the Lévy jump depend only on the derivative of the potential at the departing position, but not on the values of the potential between the departing position and the arriving position. Thus, finite size Lévy jumps allow a particle to overcome any potential barrier, even an infinite one. Here we will show that this produces a remarkable effect, which is that the current does not vanish in the limit of infinite V_0. The result is rather counterintuitive and, as we discuss later, it would be considered unphysical unless an appropriate interpretation of the model is given.

To see that the current does not vanish in the $V_0 \to \infty$ limit we can follow the same procedure used in section 3 for analyzing the limit $\sigma \to 0$. Note that, for $V_0 \to \infty$ we expect that the stationary distribution $P_{\rm s}(x)$ equals $\delta(x - x_{\min})$ regardless of the value of σ. Then, the probabilities P_k for k-wells escapes (i.e. a jump through $|k|$ successive infinite potential barriers) will be given exactly by equation (16), now with an arbitrary value of σ. Moreover, the contribution to the current of a k-well escape will be given exactly by $kL/\mathrm{d}t$. Thus, the current should be given exactly by the $\mathrm{d}t \to 0$ limit of the right-hand side of equation (14), with P_k given by equation (16). This leads to the same formula found in equation (18), which, as previously indicated, does not depend on the parameter V_0.

In figure 7 we show the current as a function of α for different values of V_0 computed with the FP formalism, together with the corresponding $V_0 \to \infty$ limit taken from equation (18). The convergence for increasing V_0 is apparent. This is quite remarkable since the Fokker–Planck results provide a completely independent calculation of the large V_0 limit.

The fact that equation (18) is found both for the large V_0 and small σ demands a careful interpretation. It is important to stress that the dynamical behavior in the two limits is not the same, since for $\sigma = 0$ we get $J = 0$ while for $V_0 \to \infty$ the current does not vanish. However, the two limits are correctly described by the same formula given in equation (18). The key point is that the formula in equation (18) is linear on σ^{α} while it does not depend on V_0. Note that the use of the formula in the two limits is somewhat different. On the one hand, the result in equation (18) has to be understood as an approximation valid for small σ that becomes exact only in the limit $\sigma = 0$, yielding $J = 0$. On the other hand, equation (18) gives us the exact result for the current in the exact $V_0 \to \infty$ limit, valid for any finite value of σ. This latter result vanishes only for

J. Stat. Mech. (2013) P02007

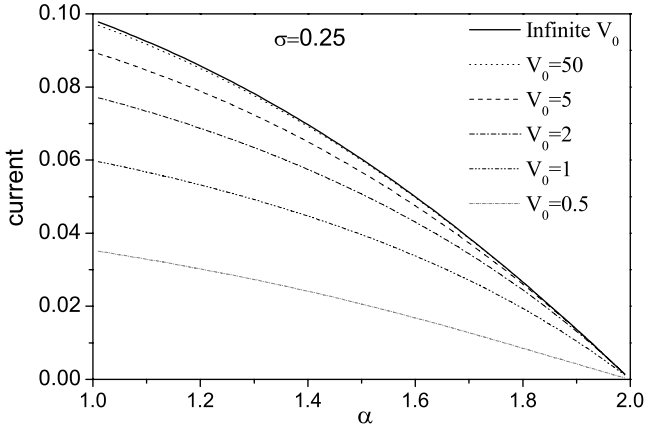

Figure 7. Current as function of α for the system with the potential defined in equation (7) for different values of V_0. The solid line shows the infinite V_0 limit calculated using equation (17) while the dashed and dotted curves show results from the FP formalism at finite V_0.

$\sigma = 0$ or for $q = 1/2$ (i.e. when the minimum of the potential is located symmetrically between two maxima).

To delve deeper into the relation between the two limits, we analyze the way in which $P_s(x)$ and J depend on the system parameters according to the Fokker–Planck theory. First, an analysis of equation (5) indicates that, for arbitrary values of the parameters, the probability distribution $P_s(x)$ depends on the parameters σ, α, V_0 and L only through the combination $\eta = \sigma^\alpha L^{2-\alpha}/V_0$. Thus, this is the parameter that should be small in order to approximate $P_s(x)$ by $\delta(x - x_{\min})$. In particular, it is easy to see from (5) that $P_s(x) = \delta(x - x_{\min})$ is the exact solution for $\eta = 0$ (i.e. $\sigma = 0$ or $V_0 \to \infty$). Second, as shown in [13], equation (6) tells us that for arbitrary values of the system parameters the current depends on σ, α, V_0 and L as

$$J = J(\sigma, \alpha, V_0, L) = g(\alpha, \eta)\frac{V_0}{L}, \tag{19}$$

where $g(\alpha, \eta)$ is an unknown function of the two parameters. This all indicates that the relevant parameters of the system are $\alpha, V_0/L$ and $\eta = \sigma^\alpha L^{2-\alpha}/V_0$, and that the solution for the current can only depend explicitly on these three parameters. Clearly, the fact that in equation (18) we find J proportional to σ^α and no dependence on V_0 indicates that $g(\alpha, \eta)$ must be linear on η at small η. Thus, we can write $g(\alpha, \eta) \simeq g_1(\alpha)\eta$, with $g_1(\alpha)$ equal to the derivative of g with respect to η evaluated at $\eta = 0$. Then, we have $J = g_1(\alpha)\eta V_0/L = g_1(\alpha)\sigma^\alpha L^{(1-\alpha)}$, which has the form of equation (18), independent of V_0. Moreover, we can recognize $g_1(\alpha)$ as equal to $k_\alpha[\zeta(\alpha, 1-q) - \zeta(\alpha, q)]$. Note that the function $g(\alpha, \eta)$ is expected to have all the information on the shape of the potential determining the current for arbitrary values of the parameters. Interestingly, we see that the first term of its Taylor expansion on η contains only the most relevant information characterizing the period and the asymmetry parameter q. If we could go further in the Taylor expansion of $g(\alpha, \eta)$ on η we could probably find the way in which the remaining information on the shape of the potential enters in the derivatives of g and affects the current at larger values of η.

J. Stat. Mech. (2013) P02007

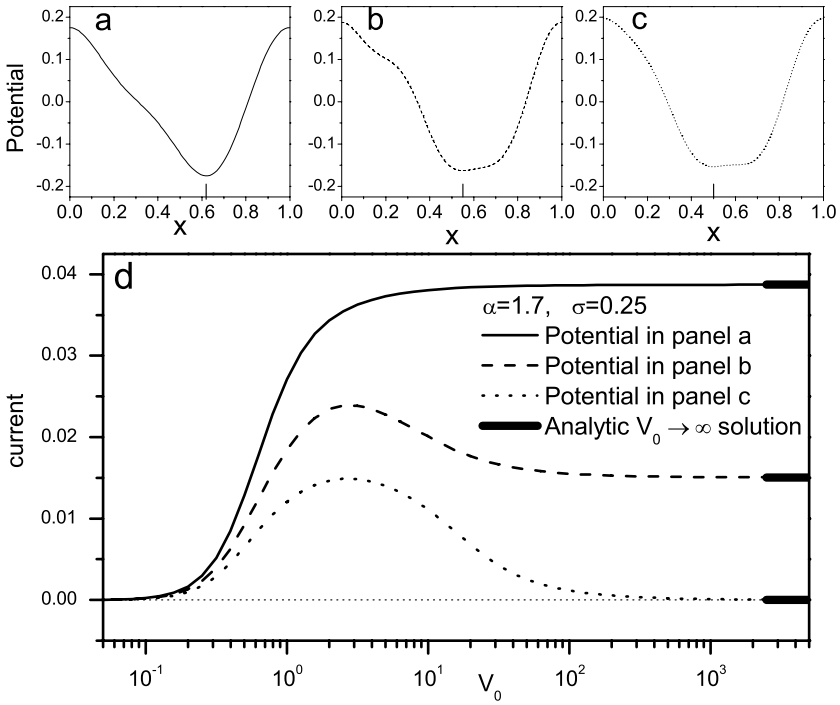

Figure 8. Current as function of V_0 for different ratchet potentials defined by equation (20). (a) Standard ratchet (see equation (7)) with minimum at $x_{\min} \simeq 0.62$ obtained from equation (20) considering $(a_1, a_2, a_3) = (0, 0, 0)$ and $(b_1, b_2, b_3) = (1/(2\pi), 1/(8\pi), 0)$. (b) Potential with minimum at $x \simeq 0.55$, parameters $(a_1, a_2, a_3) = (0.1547, 0.017, 0.0153)$, $(b_1, b_2, b_3) = (0.0816, -0.0136, -0.0187)$. (c) Potential with minimum at $x \simeq 0.55$, parameters $(a_1, a_2, a_3) = (0.175, 0.021\,875, 0)$, $(b_1, b_2, b_3) = (0.0525, 0, -0.0175)$. In all cases, the position of the minimum is indicated with a small vertical segment on the x axis. (d) Current as function of V_0 for the various potentials computed with FP theory. The segments on the right indicate the analytic infinite-V_0 result for the different potentials.

Now we briefly analyze the dependence of J on α for different values of the asymmetry parameter q. For this, we consider equation (1) with the three different potentials shown in figures 8(a)–(c). All three potentials have the same amplitude and are defined by the general three-mode formula

$$V_F(x) = V_0 \sum_{n=1}^{3} a_i \cos(2n\pi(x + x_0)) + b_i \sin(2n\pi(x + x_0)), \tag{20}$$

with the coefficients indicated in the figure 8 caption and x_0 appropriately defined to shift the position of the maxima to integer values. The potential in figure 8(a) is the standard ratchet of equation (7), which has its minimum at $x \simeq 0.62$ (this means $q \simeq 0.62$ since we have $L = 1$). The one in figure 8(b) has its minimum at $x = q \simeq 0.55$ so that its asymmetry is weaker. Finally, the potential in figure 8(c) is minimum at $x = q = 0.5$. Note that, in this latter case, the anisotropy of the potential is not due to an asymmetry in the position of the minimum with respect to the maxima, but only to the curvatures.

J. Stat. Mech. (2013) P02007

In figure 8(d) we show the current as a function of V_0 for the three potentials. We see that only the potential in figure 8(a) produces a monotonic growth of the current with the barrier height. In contrast, for the other two potentials, the current decreases at large V_0. However, only the potential with $q = 1/2$ leads to a vanishing current for $V_0 \to \infty$. Note that, in the three cases, the $V_0 \to \infty$ limit is given by the equation (18) considering the appropriate value of q. Finally, we can see that for any value of V_0 the current decreases when the parameter q approaches the value 0.5, as was shown to occur for a fixed V_0 in [5].

The peculiarity of the result studied in this section demands some discussion on the possible applications of the Lévy ratchet model. Note that, in case that the model was used to describe a particular physical system with the variable x representing the position of a particle, the *tunneling*-like effect through an infinite barrier would be considered unphysical, unless appropriate interpretations of the model and their limitations were given. But note that also the discontinuities on the trajectories occurring for any value of V_0 would require some interpretation. The model would make sense, for instance, if the long Lévy jumps account for the existence of sudden large impulses with forces surpassing those from the external potential. Another possibility is that large jumps represent the action of an alternative transport mechanism which temporally suppress the action of the potential. In other contexts where x does not represent the position of a particle, the Lévy ratchet model may be used with many different interpretations.

5. Discussion and conclusions

In this paper we have analyzed the properties of the Lévy jumps in the Lévy ratchet as well as their role in determining the directional motion.

Our results show that in the parameter region where the current is appreciable (i.e. intermediate values of σ) the escapes from a potential well depart mainly from two zones. Namely, the region close to the minimum of the potential (where the probability of finding the particle is large), and the zones close to the maxima of the potential (from where there is a high likelihood that short impulses can take the particle out). We have found that the current is sustained mainly due to the contribution of the large escapes departing from the zone around the minimum of the potential, since left and right short escapes departing from zones close to the maxima of the potential average out. Thus, we can say that only long jumps are capable of taking advantage of the asymmetry of the potential. Note that the asymmetry between the distances from the minimum of the potential to the left and right maxima induce a larger probability of escaping to the side of the nearest maximum. However, we have seen that such a kind of strong asymmetry is not essential for observing a non-vanishing current (except in the $\sigma \to 0$ and $V \to \infty$ limits, as equation (17) indicates). In fact, in section 4 we have shown an example of a potential in which the minimum is equidistant from the two maxima and a non-null current emerges, probably due to the asymmetry of the curvatures of the potential. This last feature deserves further analysis.

In the Gaussian-noise limit $\alpha = 2$, the large escapes departing from zones close to the minimum of the potential cease to exist and only small escapes departing from zones around the maxima occur, producing no effective current.

Concerning the lengths of the escapes determining the current in a standard ratchet, we have shown that the strongest asymmetry between left and right escapes occurs in one-

J. Stat. Mech. (2013) P02007

well length jumps. In fact, by considering the contribution of left and right one-well jumps we can construct a good approximation for the current which, although systematically underestimated, shows the same J-versus-σ profile as the actual current and is quite good at small σ. However, our results indicate that, except for small values of σ, the contribution of larger Lévy jumps is not negligible. For instance, in order to provide an accurate approximation for the current in the main zone of intermediate values of σ where the current is maximized, we need to consider up to 6-well jumps for $\alpha = 1.7$ and up to 10-well jumps for $\alpha = 1.3$.

In the last part of the paper we have analyzed the dependence of the current on the amplitude of the potential barrier and we have shown that standard Lévy ratchets produce a non-vanishing current even in the infinite-barrier limit. We have discussed the relevance of this rather counterintuitive result for physical models as well as the relation between the infinite-barrier limit and the $\sigma \to 0$ limit.

Acknowledgments

The authors acknowledge A B Kolton for interesting discussion and support from CNEA and from CONICET under Grant No. PIP 11220080100076.

References

[1] Reimann P, 2002 *Phys. Rep.* **361** 57
[2] Hänggi P and Marchesoni F, 2009 *Rev. Mod. Phys.* **81** 387
[3] Chowdhury D, Schadschneider A and Nishinari K, 2005 *Phys. Life Rev.* **2** 318
[4] Dybiec B, Gudowska-Nowak E and Sokolov I M, 2008 *Phys. Rev.* E **78** 011117
[5] del-Castillo-Negrete D, Gonchar V Yu and Chechkin A V, 2008 *Physica* A **387** 6693
[6] Samorodnitsky G and Taqqu M S, 1994 *Stable Non-Gaussian Random Processes* (New York: Chapman and Hall)
Applebaum D, 2004 *Lévy Processes and Stochastic Calculus* (Cambridge: Cambridge University Press)
[7] Dybiec B, 2008 *Phys. Rev.* E **78** 061120
[8] Bouzat S, 2010 *Physica* A **389** 3933
[9] Pavlyukevich I, Dybiec B, Chechkin A V and Sokolov I M, 2010 *Eur. Phys. J. Spec. Top.* **191** 223
[10] Kullberg A and del Castillo Negrete D, 2012 *J. Phys. A: Math. Theor.* **45** 255101
[11] Ai B-Q and He Y-F, 2010 *J. Stat. Mech.* P04010
[12] Ai B-Q and He Y-F, 2010 *J. Chem. Phys.* **132** 094504
[13] Ibáñez S A, Kolton A B, Risau-Gusman S and Bouzat S, 2011 *J. Stat. Mech.* P08025
[14] Imkeller P and Pavlyukevich I, 2006 *J. Phys. A: Math. Gen.* **39** L237
[15] Imkeller P and Pavlyukevich I, 2006 *Stoch. Process. Appl.* **116** 611
[16] Podlubny I, 1999 *Fractional Differential Equations* (London: Academic)

J. Stat. Mech. (2013) P02007